Translesion DNA Synthesis by Human DNA Polymerase η on Templates Containing a Pyrimidopurinone Deoxyguanosine Adduct, 3-(2′-Deoxy-β-D-*erythro*-pentofuranosyl)pyrimido-[1,2-*a*]purin-10(3*H*)-one†

Jennifer B. Stafford,‡ Robert L. Eoff,‡ Albena Kozekova,§ Carmelo J. Rizzo,§ F. Peter Guengerich,‡ and Lawrence J. Marnett*,‡,§

Departments of Chemistry and Biochemistry, A. B. Hancock, Jr., Memorial Laboratory for Cancer Research, Center in Molecular Toxicology, Vanderbilt-Ingram Cancer Center, Vanderbilt University School of Medicine, Nashville, Tennessee 37232

Received August 24, 2008; Revised Manuscript Received November 13, 2008

ABSTRACT: M_1dG (3-(2′-deoxy-β-D-*erythro*-pentofuranosyl)pyrimido[1,2-*a*]purin-10(3*H*)-one) lesions are mutagenic in bacterial and mammalian cells, leading to base substitutions (mostly M_1dG to dT and M_1dG to dA) and frameshift mutations. M_1dG is produced endogenously through the reaction of peroxidation products, base propenal or malondialdehyde, with deoxyguanosine residues in DNA. The mutagenicity of M_1dG in *Escherichia coli* is dependent on the SOS response, specifically the umuC and umuD gene products, suggesting that mutagenic lesion bypass occurs by the action of translesion DNA polymerases, like DNA polymerase V. Bypass of DNA lesions by translesion DNA polymerases is conserved in bacteria, yeast, and mammalian cells. The ability of recombinant human DNA polymerase η to synthesize DNA across from M_1dG was studied. M_1dG partially blocked DNA synthesis by polymerase η. Using steady-state kinetics, we found that insertion of dCTP was the least favored insertion product opposite the M_1dG lesion (800-fold less efficient than opposite dG). Extension from M_1dG·dC was equally as efficient as from control primer-templates (dG·dC). dATP insertion opposite M_1dG was the most favored insertion product (8-fold less efficient than opposite dG), but extension from M_1dG·dA was 20-fold less efficient than dG·dC. The sequences of full-length human DNA polymerase η bypass products of M_1dG were determined by LC-ESI/MS/MS. Bypass products contained incorporation of dA (52%) or dC (16%) opposite M_1dG or −1 frameshifts at the lesion site (31%). Human DNA polymerase η bypass may lead to M_1dG to dT and frameshift but likely not M_1dG to dA mutations during DNA replication.

Oxidation of biological macromolecules generates reactive electrophiles that chemically modify DNA. Adducts resulting from the reaction of DNA with endogenously produced electrophiles, like malondialdehyde (MDA)[1] and base propenals, may play a role in mutagenesis and carcinogenesis. MDA is produced endogenously as a byproduct of lipid peroxidation and prostaglandin biosynthesis and reacts with deoxyguanosine (dG), deoxyadenosine (dA), and deoxycytidine (dC) in DNA at physiological pH (*1*−*5*). Reaction with dG results from the addition of MDA to N^2 and N1 to form M_1dG (3-(2′-deoxy-β-D-*erythro*-pentofuranosyl)pyrimido[1,2-*a*]purin-10(3*H*)-one, Figure 1). Whereas formation of M_1dG is the major product of MDA reaction with DNA, reactions with dA and dC occur at lower levels than with dG, and adduction occurs at the exocyclic nitrogen without cyclization. The

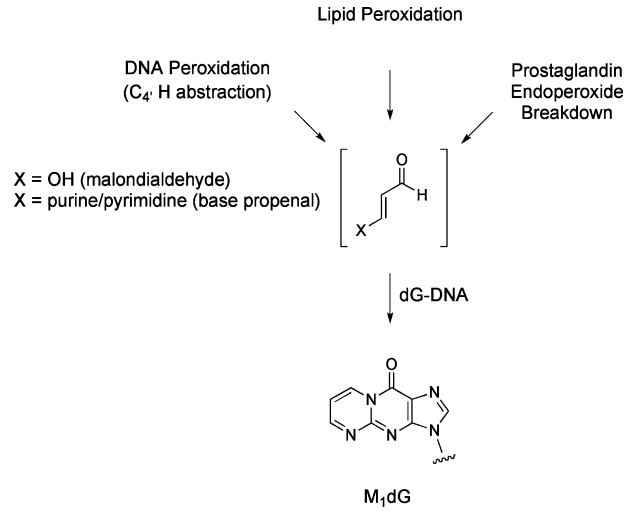

FIGURE 1: Formation and structure of M_1dG.

† This work was supported by NIH Grants R37-CA087819 (L.J.M.), RO1-ES1037 (C.J.R.), P30-ES05355 (C.J.R.), P30-ES00267 (C.J.R.), ROI-ES010375 (F.P.G.), P30-ES000267 (F.P.G.), and F32-CA119776 (R.L.E.).

* To whom correspondence should be addressed at the Department of Biochemistry, Vanderbilt University School of Medicine. E-mail: larry.marnett@vanderbilt.edu. Telephone: 615-343-7329. Fax: 615-343-7534.

‡ Department of Chemistry, Vanderbilt University School of Medicine.

§ Department of Biochemistry, Vanderbilt University School of Medicine.

[1] Abbreviations: MDA, malondialdehyde; M_1dG, 3-(2′-deoxy-β-D-*erythro*-pentofuranosyl)pyrimido[1,2-*a*]purin-10(3*H*)-one; γ-HOPdG, γ-hydroxy-1,N^2-propano-2′-deoxyguanosine; dG, deoxyguanosine; dA, deoxyadenosine; dC, deoxycytosine; dT, thymidine; DTT, dithiothreitol; BSA, bovine serum albumin; MOPS, morpholinopropanesulfonic acid; pol η, human DNA polymerase η; PdG, 1,N^2-propano-2′-deoxyguanosine; dNTP, deoxynucleoside triphosphate; LC-ESI/MS/MS, liquid chromatography−electrospray ionization/tandem mass spectrometry; CID, collision-induced dissociation; TIC, total ion chromatogram.

10.1021/bi801591a CCC: $40.75
Published on Web 12/24/2008

major endogenous source for M_1dG formation is likely through the reaction of dG with base propenals generated during DNA oxidation (*6*−*8*). As structural analogues of MDA, base propenals produced by agents such as bleomycin and peroxynitrite are more highly reactive under physiologic conditions to electrophilic DNA addition than MDA and are more mutagenic (*6, 7*).

M_1dG is a mutagenic DNA lesion in bacterial and mammalian cell culture studies (*9*−*14*), and M_1dG has been detected in DNA isolated from normal rat and human liver (*15, 16*). The profile of the *in vitro* chemical reactivity of MDA with DNA parallels the mutations observed when single-stranded M13 phage DNA is randomly modified with MDA and replicated in *Escherichia coli* (*3*−*5, 11*). The majority of observed mutations were base pair substitutions (76% of all mutations, mostly dG to dT with fewer dC to dT and dA to dG) and frameshift mutations (16% of all mutations) (*11*). Site-specific mutagenesis was used to determine the biological results of bacterial and mammalian cell replication of DNA containing M_1dG at a defined location in DNA (*13*). Base pair substitutions (mostly M_1dG to dT and M_1dG to dA) were observed in all cases, and frameshift mutations occurred when M_1dG was placed within CpG repeat sequences. Similar results were obtained with the M_1dG structural analogue, 1,N^2-propano-2′-deoxyguanosine (PdG) (*17*).

The biochemical basis for mutations resulting from unrepaired M_1dG in DNA may result from errors in DNA replication by polymerases. Many DNA lesions stall DNA replication by high-fidelity DNA polymerases. In *E. coli*, stalling of DNA replication induces a set of genes that function to repair and/or bypass the DNA damage (SOS response). Both SOS response-inducible DNA polymerase IV (dinB) and DNA polymerase V (UmuD′$_2$C) are capable of bypassing DNA lesions (*18*). M_1dG blocks *in vitro* DNA replication by processive polymerases, and M_1dG- and PdG-induced mutations in bacteria are dependent on induction of the SOS response (*11, 17, 19*−*22*). Additionally, base pair substitution mutations in replicated PdG-containing DNA are significantly reduced in *E. coli* lacking functional UmuC or UmuD proteins. These results suggest that the SOS-induced DNA polymerase V may bypass M_1dG and PdG lesions and contribute to mutagenesis through DNA replication-dependent errors (*23*).

The general mechanisms of translesion DNA synthesis are conserved between *E. coli*, yeast, and mammalian cells (*18, 24*). Mammalian cells contain at least five DNA polymerases that replicate past lesions in DNA (DNA polymerases η, ι, κ, ζ, and Rev1). In addition, DNA polymerase V and DNA polymerase η may have functional and structural homology (*25*). In mammalian cells, a variety of targeted and untargeted mutations were detected in site-specific mutagenesis studies using M_1dG, suggesting that error-prone DNA replication may also significantly contribute to mutagenesis in mammalian cells (*13*). Both yeast and human DNA polymerase η (pol η) bypass PdG and acrolein-adducted deoxyguanosine *in vitro* (*26, 27*). However, it is not known whether mammalian translesion DNA polymerases bypass M_1dG lesions *in vitro* and whether lesion bypass may lead to base pair substitutions or frameshift mutations during DNA replication. To address this possibility, we examined the capacity for human DNA polymerase η to synthesize DNA across from an M_1dG lesion placed in an oligodeoxynucleotide.

MATERIALS AND METHODS

Materials. Recombinant human DNA polymerase η (Enzymax, Lexington, KY) was aliquoted into 5 μL portions and stored at −80 °C. T4 polynucleotide kinase and *E. coli* uracil DNA glycosylase were obtained from New England Biolabs (Beverly, MA). [γ-^{32}P]ATP was purchased from Perkin-Elmer. PAGE−urea gel reagents were purchased from National Diagnostics, Inc. (Atlanta, GA).

Oligonucleotide Synthesis. The modified oligonucleotides was synthesized by a postsynthetic modification strategy as described previously and purified by HPLC (*28*). The oligonucleotide sequence was 5′-TCA CXG AAT CCT TAC GAG CCC CC-3′, where X = dG or M_1dG. The theoretical MALDI-TOF MS (HPA) *m*/*z* for the (M − H) ion of the oligonucleotide was 6977.1 and was experimentally determined to be 6976.9.

Generation of Primer-Template DNA for in Vitro Experiments. The 18-base primer oligonucleotides, 5′-GG GGG CTC GTA AGG ATT C-3′, were 5′-phosphorylated with T4 polynucleotide kinase with 250 μCi of [γ-^{32}P]ATP (>6000 Ci/mmol) in the presence of 50 mM MOPS, pH 7.5, 10 mM $MgCl_2$, and 5 mM DTT for 1 h at 37 °C. The ^{32}P-labeled primers were mixed with M_1dG-containing or control template in a 1:1 molar ratio in the presence of 40 mM NaCl and heated to 95 °C for 2 min, followed by slow cooling overnight.

Steady-State Kinetics. Human pol η stocks were diluted in reaction buffer containing 50 mM MOPS, pH 7.5, 5 mM DTT, 0.01 mg/mL BSA, and 10% glycerol (v/v). Typical reaction volumes of 10 μL contained 50 nM annealed, 5′-end-labeled primer-template, 1.6 nM human pol η, 5 mM $MgCl_2$, and 1 nM to 1 mM individual nucleoside triphosphates in reaction buffer. Enzyme, buffer, and DNA template were preincubated at 37 °C for 5 min prior to the addition of $MgCl_2$ and dNTP to initiate the reaction. The reaction incubation periods were optimized to ensure that the data collected represented initial velocities of the reactions. Reactions were terminated by the addition of 10 μL of 95% formamide, 10 mM EDTA, 0.03% bromophenol blue (w/v), and 0.03% xylene cylanol (w/v). Reactions were then heated to 95 °C for 2 min to ensure reaction quenching. Products were visualized on 20% polyacrylamide−urea gels by electrophoresis at a constant voltage (3000 V) for 3 h. Gels were exposed to phosphorimager analysis and quantified using the Bio-Rad Image Quant software. Data represent the mean and standard deviation of three experiments.

Primer Extension Analysis. Reactions were conducted in reaction buffer with 5 mM $MgCl_2$, 50 nM template, and varying amounts of human pol η enzyme for 30 min. Products were visualized on 20% polyacrylamide−urea gels followed by phosphorimager quantitation.

LC-ESI/MS/MS Analysis of Oligonucleotide Products from Human DNA Polymerase η. Templates were primed with the sequence 5′-GG GGG CTC GTA AGG ATU C-3′ for use in LC-ESI/MS/MS analysis (*29*). Human pol η (160 nM) was incubated with 1 nmol (10 μM) of annealed primer-template for 4 h at 37 °C in the presence of 5 mM $MgCl_2$, dNTPs (1 mM each), 50 mM MOPS, pH 7.5, 5 mM DTT,

0.01 mg/mL BSA, and 10% glycerol (v/v). The reaction was terminated by extraction of unused dNTPs by size exclusion on a Sephadex G-25 column. Concentrated buffer was added to restore the buffer concentrations to 20 mM Tris-HCl, pH 8.0, 1 mM DTT, and 1 mM EDTA. The reactions were initiated by the addition of 20 units of uracil DNA glycosylase and were incubated at 37 °C for 6 h to hydrolyze the uracil residue on the extended primer. The reaction mixture was then incubated at 95 °C for 1 h in the presence of 0.25 M piperidine. Solvents were removed by vacuum centrifugation, and the reaction mixture was resuspended in 100 μL of H_2O for LC-ESI/MS/MS analysis.

LC-ESI/MS/MS analysis was conducted on a Waters Acquity ultraperformance liquid chromatography system connected to a Finnigan LTQ mass spectrometer (ThermoElectron Corp., San Jose, CA). Negative ion electrospray ionization was used with a source voltage of 4 kV, source current 100 μA, auxiliary gas flow rate setting 20, sweep gas flow rate setting 5, sheath gas flow setting 34, and capillary voltage −90 V. Buffer A contained 10 mM $NH_4CH_3CO_2$ plus 2% CH_3CN, and buffer B contained 10 mM NH_4CH_3CO plus 95% CH_3CN. Using a flow rate of 150 μL/min and an Acquity ultraperformace liquid chromatography BEH octadecysilane (C_{18}) column (1.7 μm, 1.0 × 100 mm) this buffer gradient program was used: 0−3 min, linear gradient from 100% A to 97% A; 3−4 min, linear gradient to 80% A; 4−5 min, linear gradient to 0% A (100% B); 5−5.5 min, hold at 100% B; 5.5−6.5 min, linear gradient to 100% A; 6.5−9.5 min, hold at 100% A. The column temperature was maintained at 50 °C. For MS/MS analysis the normalized collision energy was 35%, activation Q 0.250, and activation time 30 ms. Nucleotide composition and CID fragmentations of oligonucleotide sequences were calculated using the Oligo composition calculator (v1.2) and the Mongo Oligo mass calculator (v.2.06), respectively, maintained by the Department of Medicinal Chemistry at the University of Utah (www.medlib.med.utah.edu/massspec).

RESULTS

Human DNA Polymerase η Replicates DNA Past the M_1dG Lesion. Primer extension studies were conducted to examine the ability of pol η to synthesize DNA across from M_1dG. M_1dG was specifically incorporated into the fifth position from the 5′-end of a 24 base pair oligonucleotide (Figure 2). Unmodified (control) templates or M_1dG-containing templates were annealed to 18-base standing start (−1) primers for use in primer extension assays. Template-primer (50 nM) was incubated with increasing concentrations of pol η at 37 °C for 30 min in the presence of all four deoxynucleoside triphosphates (dNTPs) (100 μM). Figure 2 illustrates the extent to which DNA synthesis occurred opposite and past the M_1dG lesion. At the highest enzyme concentrations used (32 nM) 72% of control templates were extended to full-length product. The M_1dG lesion blocked incorporation of the initial nucleotide opposite the lesion, but 14% of templates were extended to full-length product. DNA replication past M_1dG appeared distributive, because the intensities of bands corresponding to subsequent base addition were approximately equal.

Steady-State Kinetic Analysis of Nucleotide Incorporation Opposite M_1dG Lesions in DNA. Control or M_1dG-containing primer-template was incubated with catalytic amounts of pol

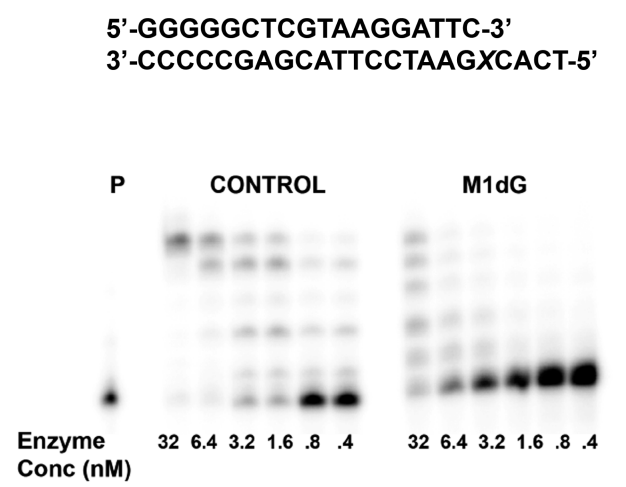

FIGURE 2: Human DNA polymerase η synthesizes DNA across from M_1dG lesions and forms fully extended DNA products. Primer extension assays were conducted using decreasing concentrations of human DNA polymerase η incubated for 30 min with 50 nM DNA primer-template. Primer-template extension is shown under conditions with no enzyme (P, primer), unmodified primer-template (control, X =dG), and M_1dG-modified primer-template (M_1dG, X = M_1dG). Samples were visualized by electrophoresis on a 20% urea-denatured PAGE.

η and varied concentrations of a single dNTP for various amounts of time. The amount of one-nucleotide-extended primer was quantified to determine the initial velocity of the enzymatic reaction. Initial velocities were plotted against the concentration of dNTP used, and nonlinear curve fit regression analysis was performed to a one-site hyperbolic curve (Figure 3). From this analysis K_m and k_{cat} values were determined (Table 1). K_m and k_{cat} values determined from analysis of the insertion of dCTP opposite dG template by pol η (Figure 3B) correlated with published data (*30*). Incorporation of dCTP opposite M_1dG was less favored, with a 126-fold higher K_m and a 7-fold lower k_{cat} than incorporation of dCTP opposite dG. Incorporation of dATP was equally as effective opposite M_1dG and dG (Figure 3C), as the k_{cat} and K_m values were approximately equal. In contrast to the incorporation of dATP opposite M_1dG or dG, both the K_m and k_{cat} were different for incorporation of dTTP and dGTP opposite to M_1dG or dG (Figure 3D,E). The k_{cat} for incorporation of dTTP opposite M_1dG was 73% lower than the k_{cat} for incorporation of dTTP opposite dG, and the K_m was approximately one-third of that for incorporation of dTTP opposite dG. Incorporation of dGTP opposite dG occurred with 2-fold higher K_m and 50% faster k_{cat} than incorporation opposite M_1dG.

Misincorporation frequencies were calculated as the ratio of k_{cat}/K_m for the incorporated nucleotide (control or M_1dG templates) to the ratio of k_{cat}/K_m for incorporation of dCTP opposite dG (Table 1) (*31*). This analysis determined that incorporation of dATP opposite the M_1dG lesion is most favored, followed by approximately equivalent efficacy of incorporation of dGTP and dTTP. Incorporation of dCTP opposite M_1dG was the least kinetically favored insertion product.

Analysis of Product Extension by Steady-State Kinetics. Replication of modified DNA requires both incorporation of a nucleotide opposite the lesion and extension of the resulting insertion product. DNA lesions and mispairs may alter the efficiency of extension of bypassed DNA lesions

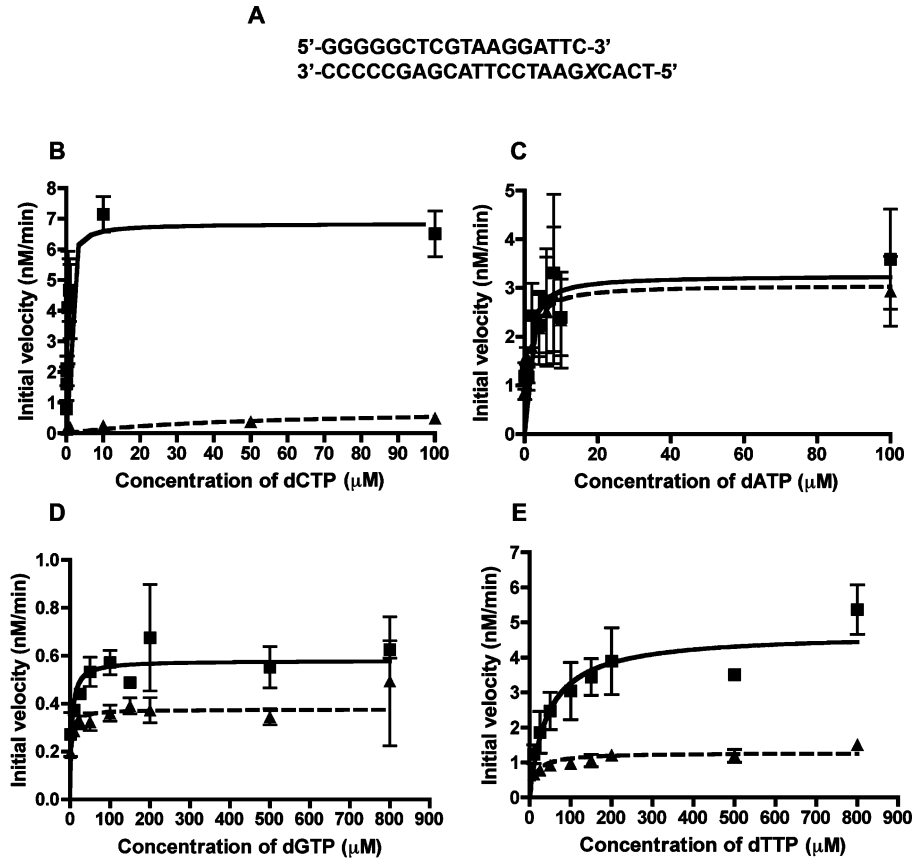

FIGURE 3: Steady-state kinetics for single nucleotide incorporation opposite the M_1dG lesion in DNA. (A) Primer-template used for single nucleotide incorporation studies: X = dG (control, squares and solid lines) or M_1dG (triangles and dashed lines). Primer-template (50 nM) was incubated with 1.6 nM human DNA polymerase η for various amounts of time in the presence of increasing concentrations of (B) dCTP, (C) dATP, (D) dGTP, or (E) dTTP. Error bars represent the standard deviation of at least three experiments. Curves were fit to a single binding site hyperbolic curve.

Table 1: Steady-State Kinetic Parameters for Insertion of Single Nucleotides Opposite Control and M_1dG-Modified Template by Human DNA Polymerase η[a]

template	dNTP	K_m (μM)	k_{cat} ($s^{-1} \times 10^3$)	k_{cat}/K_m (μM^{-1} $s^{-1} \times 10^{-3}$)	f (misinsertion frequency)[b]
dG	C	0.4 ± 0.1	71 ± 1	180	1
	A	2.3 ± 0.7	57 ± 2	25	0.13
	T	40 ± 20	48 ± 4	1	0.006
	G	4 ± 2	5.9 ± 0.4	1.4	0.007
M_1dG	C	50 ± 20	8.2 ± 0.8	0.2	0.0009
	A	2.4 ± 0.8	55 ± 4	23	0.12
	T	14 ± 5	13 ± 1	0.94	0.0050
	G	3 ± 2	3.9 ± 0.2	1.4	0.007

[a] Human DNA polymerase η (1.6 nM) was incubated with 50 nM control (dG) or M_1dG-containing templates in the presence of increasing concentrations of individual dNTPs for various amounts of time. The initial velocities for the insertion of individual dNTPs were determined and graphed against the concentration of dNTP to determine k_{cat} and K_m values. [b] The frequencies of misincorporation were calculated relative to insertion of dCTP opposite control (dG) primer-templates as the ratio $(k_{cat}/K_m)_{dNTP}/(k_{cat}/K_m)_{dCTP,control}$.

or mispairs when compared to nondamaged or properly matched DNA (*32, 33*). To determine if pol η extends M_1dG-modified primer-templates with altered efficacy, primers terminating with dC or dA were annealed to templates containing control (dG) or lesion (M_1dG). The efficacy of extension from these templates was measured by determining the kinetic parameters for incorporation of the next correct nucleotide (dG) to each primer-template combination (Figure 4). Extension of M_1dG·dC pairs occurred with reduced k_{cat} and K_m when compared to the extension of dG·dC pairs. However, the reduction in k_{cat} balanced the reduction in K_m, and the overall efficiency of extension for dG·dC and M_1dG·dC pairs was nearly equivalent (Table 2). By contrast to the extension of dG·dC and M_1dG·dC pairs, the extension of both dG·dA and M_1dG·dA mispairs proceeded with greatly reduced k_{cat} values, resulting in 50- and 20-fold reduced efficiency of extension, respectively (Table 2). These results suggest that pol η may extend "correctly" bypassed M_1dG lesions (M_1dG·dC) more efficiently than "mutagenically" bypassed lesions (M_1dG·dA) and equally as well as extension from undamaged templates. Extension of M_1dG·dG pairs proceeds most efficiently when pol η inserts dTTP opposite the dA residue at the +2 position, which represents the generation of a −1 frameshift deletion (Table 2). Extension of M_1dG·dG pairs by insertion of the next correct base (dGTP) is less efficient than the event that corresponds to a −1 frameshift deletion.

LC-ESI/MS/MS Analysis of Full-Length Bypass Products. To fully characterize the effects of DNA template modifications on primer extension by pol η, it is necessary to determine the sequences of full-length DNA products synthesized by the enzyme in the presence of all four dNTPs. The products of primer extension from control and M_1dG-modified template-primers were identified using an LC-ESI/MS/MS-based approach. Primer-templates were incubated at 37 °C with pol η for 4 h in the presence of all four dNTPs to generate full-length bypass products for sequence deter-

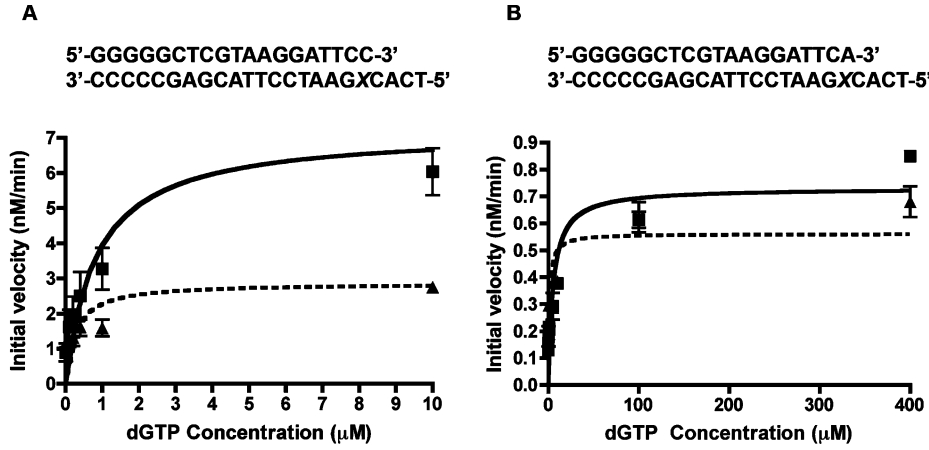

FIGURE 4: Steady-state kinetics for incorporation of dGTP immediately following the M_1dG lesion site. The extension of $M_1dG\cdot dC$ or $M_1dG\cdot dA$ paired primer-templates by human DNA polymerase η was analyzed by steady-state kinetics. Increasing concentrations of dGTP were incubated human DNA polymerase η (1.6 nM) and 50 nM (A) $M_1dG\cdot dC$ primer-templates (X = M_1dG, triangles and dashed lines) or $dG\cdot dC$ primer-templates (X = dG, squares and solid lines) or (B) $M_1dG\cdot dA$ (X = M_1dG, triangles and dashed lines) or $dG\cdot dA$ primer-templates (X = dG, squares and solid lines).

Table 2: Steady-State Kinetic Parameters for One-Base Extension of Control and M_1dG-Containing Templates by Human DNA Polymerase η[a]

template	mismatch	K_m (μM)	k_{cat} ($s^{-1} \times 10^{-3}$)	k_{cat}/K_m ($\mu M^{-1}\ s^{-1} \times 10^{-3}$)	f (misinsertion frequency)[b]
dG	dG·dC	0.8 ± 0.3	75 ± 7	90	1
	dG·dA	5 ± 2	7.6 ± 0.6	1.4	0.02
	dG·dT	1.1 ± 0.2	24 ± 1	22	0.2
	dG·dG	3 ± 1	13 ± 1	4	0.04
M_1dG	$M_1dG\cdot dC$	0.26 ± 0.09	29 ± 2	110	1.2
	$M_1dG\cdot dA$	1.2 ± 0.5	5.8 ± 0.6	4.8	0.053
	$M_1dG\cdot dT$	10 ± 5	3.5 ± 0.2	0.35	0.0032
	$M_1dG\cdot dG$				
	(dGTP)	3 ± 1	37 ± 1	12.3	0.11
	(dTTP)	0.77 ± 0.06	83 ± 2	108	1.2

[a] Human DNA polymerase η (1.6 nM) was incubated with 50 nM primer-templates pairing dC, dA, dT, or dG with control (dG) or M_1dG-containing templates and varied concentrations of dGTP (or dTTP for the $M_1dG\cdot dG$ pair) for 5 min. The initial velocities of incorporation of dNTP (next base addition) were determined and graphed against the concentration of dGTP to determine k_{cat} and K_m values. [b] The frequencies of misincorporation were calculated relative to insertion of dNTP following $dC\cdot dG$ primer-templates as the ratio $(k_{cat}/K_m)_{mismatch}/(k_{cat}/K_m)_{dG\cdot dC}$.

mination. A uracil residue was placed two bases from the 3′-end of the primer strand, and reaction products were digested with uracil DNA glycosylase and hydrolyzed with piperidine to reduce the products to a size manageable for LC-ESI/MS/MS sequence analysis.

Two major products were seen for the extension of control DNA corresponding to ions with *m/z* of 1086.7 (doubly charged ion) and 724.2 (triply charged ion) and *m/z* of 1243.7 (doubly charged ion) and 828.6 (triply charged ion). These two products corresponded to correct full-length extension of the primer-template and "blunt-end" addition of dA following correct full-length extension (Figure S1). The complete list of theoretical and observed CID fragments for the two products generated using control DNA as the template for pol η extension is found in Table S1. Approximately 69% of the product was extended correctly, and 31% of the product contained the "blunt-end" dA addition to the full-length product (Figure S1). "Blunt end" addition of dA to full-length products by pol η has been previously observed (*34*).

The substitution of M_1dG for dG resulted in four major products. The major ions observed in the total mass spectrum resulted from one product with *m/z* of 1098.7 (doubly charged ion) and 732.2 (triply charged ion), a second with *m/z* of 1087.2 (doubly charged ion) and 724.5 (triply charged ion), a third with *m/z* 942.2 (doubly charged ion), and a fourth with *m/z* of 836.5 (doubly charged ion) (Figure 5B). Sequence assignments were made based on CID fragmentation patterns. The strong signal-to-noise ratio of the CID spectra indicated that the *in vitro* polymerase reaction had proceeded with good yield. The major product (*m/z* of 1098.7 and 732.2) corresponded to the incorporation of dA opposite M_1dG (5′-pTCAGTGA-3′, Figure 5C and Table S2). Incorporation of dC opposite M_1dG (*m/z* 1087.2 and 732.2, 5′-pTCCGTGA-3′) was also observed and had a nearly identical CID fragmentation pattern as observed for the major product of control reactions (Figure 5D and Table S2). Minor products were also observed and included incorporation of dA opposite M_1dG with "blunt-end" addition of dA (*m/z* 836.5, Figure 5F and Table S2) or dG (*m/z* 1263.2, CID data not shown). Incorporation of dT or dG opposite M_1dG was not observed.

In addition to incorporation of dA and dC opposite M_1dG, a frameshift product was also observed (*m/z* 942.2) in which no nucleotide was incorporated opposite M_1dG, but the enzyme continued to generate a fully extended product. The DNA sequence of the frameshift product was confirmed by CID fragmentation in which all of the theoretical a-B and w ions were observed corresponding to the DNA sequence 5′-pTC^GTGA-3′ (Figure 5E and Table S2).

Approximate product ratios for full-length bypass of M_1dG by pol η were determined by integration of the product peak areas from the selected ion current traces for each of the four products (Figure 6). Approximately 83% of the total

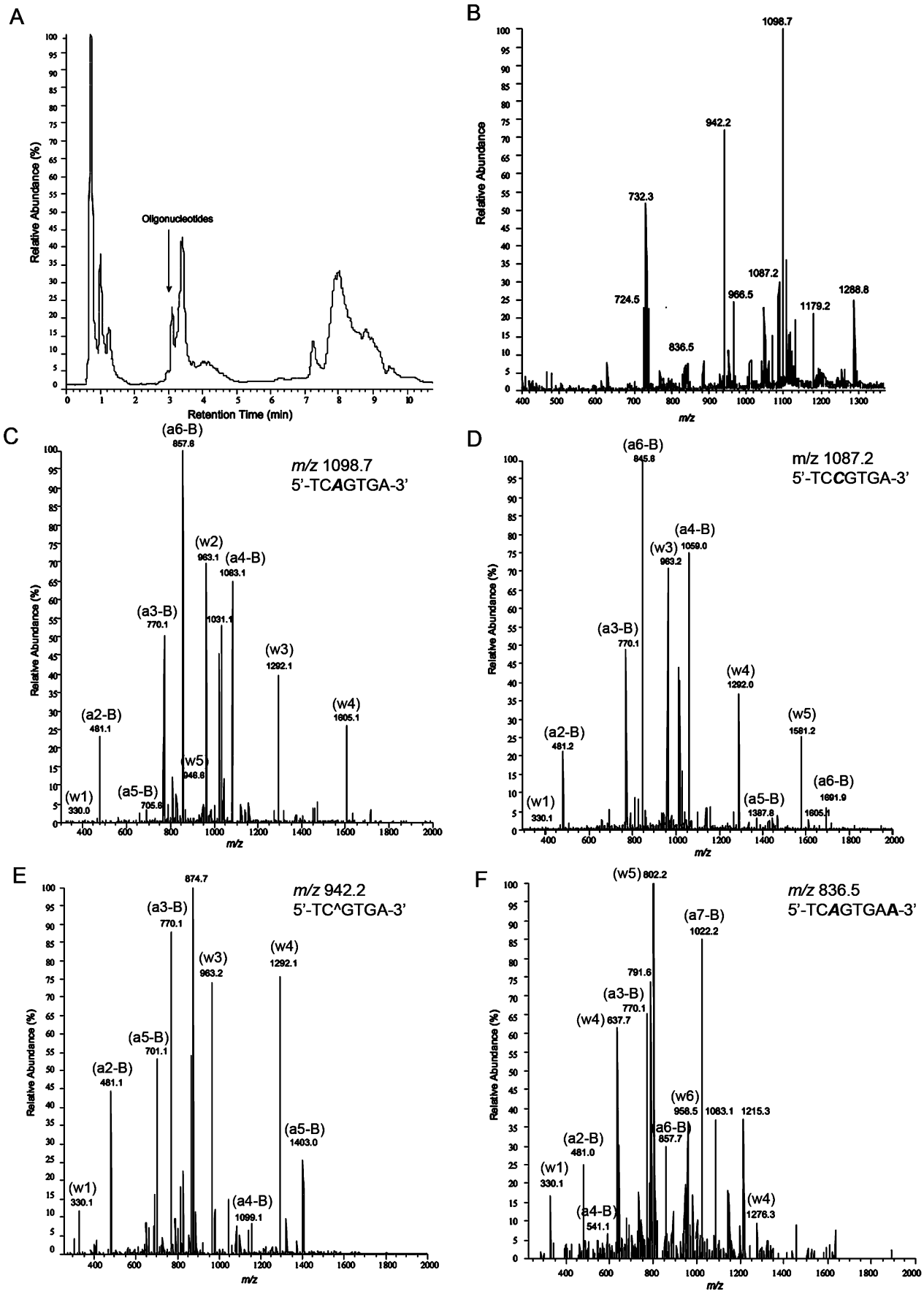

FIGURE 5: LC-ESI/MS/MS analysis of products from the *in vitro* replication of M_1dG containing DNA templates by human DNA polymerase η. (A) Total ion current trace. (B) Total mass spectrum of the mixture of M_1dG bypass products. (C) CID spectrum of *m/z* 1098.7 with sequence TC***A***GTGA. (D) CID spectrum of *m/z* 1087.2 with sequence TC***C***GTGA. (E) CID spectrum of *m/z* 942.2 with sequence TC^GTGA. (F) CID spectrum of *m/z* 836.5 with sequence TC***A***GTGAA. DNA bases shown in bold italic were incorporated opposite M_1dG lesions in the template DNA.

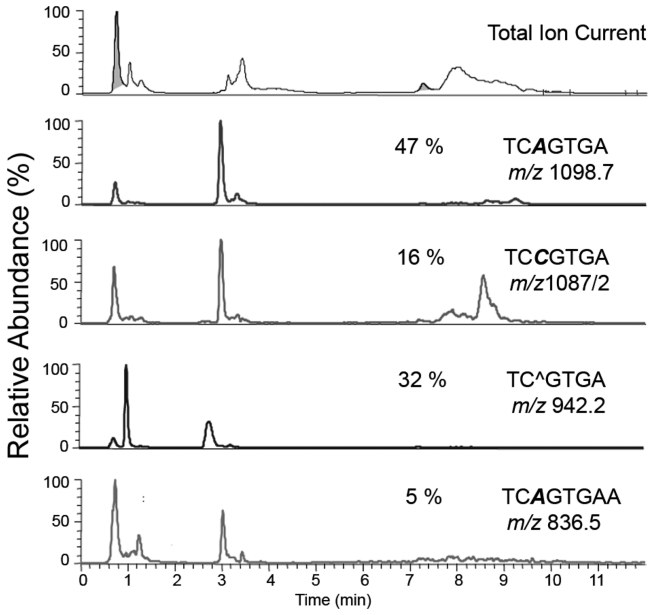

FIGURE 6: Relative abundance of M_1dG bypass products. The total ion current trace is shown with selected ion current traces for the four major M_1dG bypass products indicated. Percentages represent the relative integrated area of product peaks analyzed in Figure 5C−F. DNA bases in bold italic represent incorporation opposite the M_1dG lesion.

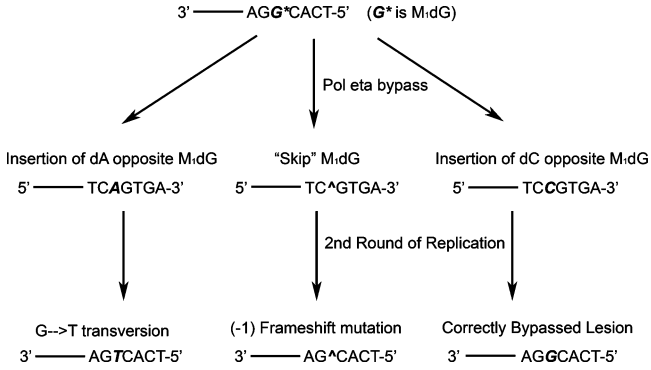

FIGURE 7: Summary of translesion bypass of M_1dG by human DNA polymerase η. The major *in vitro* products of human DNA polymerase η bypass of M_1dG lesions in DNA include insertion of dC or dA opposite the lesion and "skipping" the lesion site. If subjected to a second round of DNA replication, these bypass products would lead to correct bypass of the lesion (M_1dG to dG), a G to T transversion (M_1dG to dT), or a −1 frameshift mutation.

products were incorrectly bypassed by pol η. Incorporation of dA opposite M_1dG accounted for 52% of the total products (including blunt-end addition of dA), and 31% of the bypass products were −1 frameshifts generated by "skipping" the lesion site. Insertion of dC opposite M_1dG accounted for 16% of the bypassed product.

DISCUSSION

Our results indicate that the major products of *in vitro* bypass of M_1dG by human pol η result from incorporation of dA opposite M_1dG. This substitution would result in an M_1dG to dT transversion upon a second round of DNA replication (Figure 7) and agrees with published findings of *in vivo* replication of M_1dG containing DNA in nonreiterated sequences by mammalian and bacterial cells and replication of MDA-treated DNA in *E. coli* (*11, 13*). Insertion of dA opposite M_1dG by human DNA pol η is 130 times more favorable kinetically than insertion of dC opposite the lesion. Insertion of dA is also 24-fold more favorable than insertion of dT and 16-fold more favorable than insertion dG opposite M_1dG.

The sequences of the full-length products of pol η M_1dG lesion bypass *in vitro* were determined using LC-ESI/MS/MS. As suggested by our kinetic data, the major product of M_1dG bypass by pol η is insertion of dA opposite M_1dG (M_1dG to dT, Figure 5). In addition, significant levels of dC insertion opposite M_1dG were also observed (M_1dG to dG, Figure 5). We quantified the relative amounts of full-length products observed in LC-ESI/MS/MS analysis by integration of the selected ion current trace for individual product ions. This method assumes that the ionization and detection efficiency of each product is equal. Since the ionization efficiencies of oligonucleotides vary based on sequence, this method is an approximation of product abundance. A ratio of 3.3:1 of dA to dC insertion opposite M_1dG was observed in the extension assays characterized by LC-ESI/MS/MS. If single nucleotide incorporation kinetics alone predicted the products of M_1dG lesion bypass, we would expect a 130:1 ratio of insertion of dA to insertion of dC opposite the lesion in the full-length products. However, we also observe that extension from $M_1dG{\cdot}dA$ primer-templates is nearly 24-fold slower than extension from $M_1dG{\cdot}dC$ primer-templates. When the kinetics of both insertion and extension are combined by multiplying the frequencies of misincorporation for the insertion of dA or dC opposite M_1dG (Table 1) with the frequencies of misincorporation for the extension of $M_1dG{\cdot}dA$ or $M_1dG{\cdot}dC$ templates (Table 2), we obtain a predicted ratio of 4.3:1 for the insertion of dA to the insertion of dC opposite M_1dG. This correlates reasonably well with the observed ratio of full-length products determined by LC-ESI/MS/MS. Kinetic analysis of the insertion and extension events predicts that −1 frameshift deletion products should occur at similar or higher levels than insertion of dA opposite M_1dG, which is slightly different from the higher levels of dA insertion products observed by LC/MS/MS. Together, these data reinforce that the sequences of full-length bypass products are determined by both the efficacy of single nucleotide insertion and the efficiency of bypassed template extension. Thus, kinetic data obtained from examination of single nucleotide insertion directly opposite the DNA lesion may not be uniformly predictive of the actual ratio of bypassed products observed in the presence of all four nucleotides.

In addition to base substitution products, pol η bypass of M_1dG generates a product (*m/z* 942.2) by "skipping" the M_1dG lesion site, which would result in a −1 frameshift after a second round of replication (Figure 7). This product is interesting because, unlike many other base modifications that result from oxidative stress, M_1dG induces frameshift mutations *in vivo* (*13, 35*). Like other translesion polymerases, pol η has an "open" active site, which can accommodate the presence of two base pairs (*36, 37*). The presence of two bases in the active site may allow for the incoming dGTP to pair with the dC present 5′ to the M_1dG lesion in the template, thus creating a −1 frameshift product. The involvement of SOS-induced polymerases and Y-family DNA polymerases in frameshift mutagenesis is documented. Mutagenicity of benzo[*a*]pyrene and *N*-2-acetylaminofluo-

rene is also SOS response-dependent. Frameshift mutagenesis by benzo[*a*]pyrene lesions requires both pol II and pol V whereas frameshifts are generated uniquely by pol II for *N*-2-acetylaminofluorene (*38, 39*). These results suggest that DNA replication by translesion DNA polymerases may be partially accountable for the replication errors that lead to the observed mutagenicity of M_1dG lesions *in vivo*. However, it is noteworthy that full-length bypass products with dT opposite M_1dG were not observed in the present study. Since M_1dG to dA mutations occur at approximately the same frequency as M_1dG to dT, other factors or polymerases may contribute to the generation of M_1dG to dA mutations *in vivo*.

In general, *in vitro* replication of adducted primer-templates by pol η are lesion-specific and depend on both the insertion of bases opposite the DNA lesion and the capacity of the enzyme to synthesize DNA past the bypassed lesion. For example, pol η preferentially inserts dA-dA opposite *cis-syn* cyclobutane pyrimidine dimers and effectively elongates only primers pairing dA with the dT of a *cis-syn* cyclobutane pyrimidine dimer leading to error-free bypass of the lesion (*30, 40*−*45*). Yeast pol η also replicates past 8-oxoguanine, preferentially inserting dC opposite the lesion and extending the new template as effectively as unmodified DNA (*46*). Human pol η inserts dC or dT with approximately equal efficacy opposite O^6-methylguanine (*34*). Human pol η also replicates past exocyclic deoxyguanosine adducts. Increasing the bulk of an alkyl or aromatic hydrocarbon moiety adducted at the N^2-position of dG reduces the ability of human pol η to replicate through and past the lesion (*47*). As adduct bulk increases, the fidelity of incorporation of dC opposite the adducted dG also decreases, and extension from the resulting primer-template is concomitantly reduced (*47*). 1,N^2-Ethenoguanine adducts are also bypassed by human pol η. The enzyme inserts dG opposite the lesion moderately more efficiently than dA or dC in single nucleotide incorporation studies, but only products resulting from insertion of dG opposite the lesion are fully extended in LC-ESI/MS/MS analysis (*48*). This contrasts with the present results obtained with the close structural analogue, M_1dG.

Studies with the exocyclic acrolein-derived deoxyguanosine adduct γ-hydroxy-1,N^2-propano-2′-deoxyguanosine (γ-HOPdG) and its structural analogues suggest that the kinetics of nucleotide insertion and next base extension by both yeast and human pol η may be influenced by ring opening of the exocyclic adduct (*26, 27, 49*). Like γ-HOPdG, M_1dG can ring-open to form N^2-(3-oxo-1-propenyl)-2′-deoxyguanosine (*50*). Ring opening of M_1dG is favored under basic conditions or when placed opposite dC in duplex DNA (*51, 52*). Lloyd and co-workers compared the kinetics of single nucleotide insertion and primer-template extension by pol η on templates containing γ-HOPdG or ring-closed (PdG) and ring-opened analogues of γ-HOPdG (*26*). Insertion of dC by pol η opposite reduced γ-HOPdG (N^2-(3-hydroxypropyl)-2′-deoxyguanosine), which mimics ring-opened γ-HOPdG, is approximately as efficient as insertion of dC opposite dG (control), whereas insertion of dC opposite γ-HOPdG is 100-fold less efficient than control. Similar to our results with M_1dG, insertion of dC opposite PdG is 1600-fold less efficient than insertion of dC opposite dG (*26*). However, in contrast to the extension of M_1dG•dC primer-templates (Figure 3 and Table 2) and reduced γ-HOPdG containing primer-templates, extension of the ring-closed PdG•dC primer-templates is significantly reduced (140-fold) compared to dG•dC primer-templates (*26*). Results similar to pol η bypass of PdG were obtained with α-hydroxypropanodeoxyguanosine, which also exists primarily in a ring-closed form in duplex DNA (*27, 53, 54*). It is proposed that ring opening of the γ-HOPdG lesion may facilitate insertion of dC opposite the lesion and extension of the dC-inserted product by permitting Watson−Crick base pairing with the adducted deoxyguanosine (*27*). It is not known whether M_1dG exists in the ring-opened or ring-closed state at primer-template termini or within the active site of pol η. However, the extremely low efficiency of dC insertion opposite M_1dG by pol η but the efficient extension of M_1dG•dC-paired insertion products makes it tempting to speculate that ring opening of M_1dG may follow dC insertion, enabling efficient extension of the 3-oxopropenyl-dG•dC mispair. It was also demonstrated that the sequential action of pol ι and pol κ or yeast Rev1 and pol could catalyze the error-free bypass and extension of the γ-HOPdG lesion *in vitro* (*55, 56*). It would be interesting to examine the bypass of the M_1dG adduct with these combinations of translesion polymerases as well.

In summary, we examined replication of M_1dG-containing DNA by recombinant human DNA polymerase η. Multiple replication bypass products were characterized that result from alterations in the kinetics of nucleotide insertion opposite the lesion and extension of lesion-bypassed templates and frameshifted bypass. Bypass of M_1dG lesions by human DNA polymerase η may lead to the generation of M_1dG to dT and frameshift but likely not M_1dG to dA mutations during DNA replication. These results may be relevant to the complex mutational profile of M_1dG replication in cells.

At least five translesion DNA polymerases are present in mammalian cells, each with unique bypass properties. It is therefore of biologic interest to determine whether the bypass of M_1dG lesions by alternate human translesion DNA polymerases leads to base substitutions that generate M_1dG to dA or contribute to M_1dG to dT and frameshift mutations that are observed when M_1dG-containing DNA is replicated *in vivo*.

SUPPORTING INFORMATION AVAILABLE

Figures containing control mass spectra and tables containing theoretical and observed CID fragmentation data. This material is available free of charge via the Internet at http://pubs.acs.org.

REFERENCES

1. Diczfalusy, U., Falardeau, P., and Hammarstrom, S. (1977) Conversion of prostaglandin endoperoxides to C17-hydroxy acids catalyzed by human platelet thromboxane synthase. *FEBS Lett. 84*, 271–274.
2. Hamberg, M., and Samuelsson, B. (1967) Oxygenation of unsaturated fatty acids by the vesicular gland of sheep. *J. Biol. Chem. 242*, 5344–5354.
3. Basu, A. K., O'Hara, S. M., Valladier, P., Stone, K., Mols, O., and Marnett, L. J. (1988) Identification of adducts formed by reaction of guanine nucleosides with malondialdehyde and structurally related aldehydes. *Chem. Res. Toxicol. 1*, 53–59.
4. Stone, K., Ksebati, M. B., and Marnett, L. J. (1990) Investigation of the adducts formed by reaction of malondialdehyde with adenosine. *Chem. Res. Toxicol. 3*, 33–38.

5. Stone, K., Uzieblo, A., and Marnett, L. J. (1990) Studies of the reaction of malondialdehyde with cytosine nucleosides. *Chem. Res. Toxicol. 3*, 467–472.
6. Dedon, P. C., Plastaras, J. P., Rouzer, C. A., and Marnett, L. J. (1998) Indirect mutagenesis by oxidative DNA damage: formation of the pyrimidopurinone adduct of deoxyguanosine by base propenal. *Proc. Natl. Acad. Sci. U.S.A. 95*, 11113–11116.
7. Plastaras, J. P., Riggins, J. N., Otteneder, M., and Marnett, L. J. (2000) Reactivity and mutagenicity of endogenous DNA oxopropenylating agents: base propenals, malondialdehyde, and N(epsilon)-oxopropenyllysine. *Chem. Res. Toxicol. 13*, 1235–1242.
8. Jeong, Y. C., Sangaiah, R., Nakamura, J., Pachkowski, B. F., Ranasinghe, A., Gold, A., Ball, L. M., and Swenberg, J. A. (2005) Analysis of M1G-dR in DNA by aldehyde reactive probe labeling and liquid chromatography tandem mass spectrometry. *Chem. Res. Toxicol. 18*, 51–60.
9. Basu, A. K., and Marnett, L. J. (1983) Unequivocal demonstration that malondialdehyde is a mutagen. *Carcinogenesis 4*, 331–333.
10. Mukai, F. H., and Goldstein, B. D. (1976) Mutagenicity of malonaldehyde, a decomposition product of peroxidized polyunsaturated fatty acids. *Science 191*, 868–869.
11. Benamira, M., Johnson, K., Chaudhary, A., Bruner, K., Tibbetts, C., and Marnett, L. J. (1995) Induction of mutations by replication of malondialdehyde-modified M13 DNA in Escherichia coli: determination of the extent of DNA modification, genetic requirements for mutagenesis, and types of mutations induced. *Carcinogenesis 16*, 93–99.
12. Riggins, J. N., and Marnett, L. J. (2001) Mutagenicity of the malondialdehyde oligomerization products 2-(3′-oxo-1′-propenyl)-malondialdehyde and 2,4-dihydroxymethylene-3-(2,2-dimethoxyethyl)glutaraldehyde in Salmonella. *Mutat. Res. 497*, 153–157.
13. VanderVeen, L. A., Hashim, M. F., Shyr, Y., and Marnett, L. J. (2003) Induction of frameshift and base pair substitution mutations by the major DNA adduct of the endogenous carcinogen malondialdehyde. *Proc. Natl. Acad. Sci. U.S.A. 100*, 14247–14252.
14. Niedernhofer, L. J., Daniels, J. S., Rouzer, C. A., Greene, R. E., and Marnett, L. J. (2003) Malondialdehyde, a product of lipid peroxidation, is mutagenic in human cells. *J. Biol. Chem. 278*, 31426–31433.
15. Chaudhary, A. K., Nokubo, M., Marnett, L. J., and Blair, I. A. (1994) Analysis of the malondialdehyde-2′-deoxyguanosine adduct in rat liver DNA by gas chromatography/electron capture negative chemical ionization mass spectrometry. *Biol. Mass Spectrom. 23*, 457–464.
16. Chaudhary, A. K., Nokubo, M., Reddy, G. R., Yeola, S. N., Morrow, J. D., Blair, I. A., and Marnett, L. J. (1994) Detection of endogenous malondialdehyde-deoxyguanosine adducts in human liver. *Science 265*, 1580–1582.
17. Fink, S. P., Reddy, G. R., and Marnett, L. J. (1997) Mutagenicity in Escherichia coli of the major DNA adduct derived from the endogenous mutagen malondialdehyde. *Proc. Natl. Acad. Sci. U.S.A. 94*, 8652–8657.
18. Woodgate, R. (1999) A plethora of lesion-replicating DNA polymerases. *Genes Dev. 13*, 2191–2195.
19. Cline, S. D., Riggins, J. N., Tornaletti, S., Marnett, L. J., and Hanawalt, P. C. (2004) Malondialdehyde adducts in DNA arrest transcription by T7 RNA polymerase and mammalian RNA polymerase II. *Proc. Natl. Acad. Sci. U.S.A. 101*, 7275–7280.
20. Hashim, M. F., Riggins, J. N., Schnetz-Boutaud, N., Voehler, M., Stone, M. P., and Marnett, L. J. (2004) In vitro bypass of malondialdehyde-deoxyguanosine adducts: differential base selection during extension by the Klenow fragment of DNA polymerase I is the critical determinant of replication outcome. *Biochemistry 43*, 11828–11835.
21. Johnson, K. A., Fink, S. P., and Marnett, L. J. (1997) Repair of propanodeoxyguanosine by nucleotide excision repair in vivo and in vitro. *J. Biol. Chem. 272*, 11434–11438.
22. Burcham, P. C., and Marnett, L. J. (1994) Site-specific mutagenesis by a propanodeoxyguanosine adduct carried on an M13 genome. *J. Biol. Chem. 269*, 28844–28850.
23. Fink, S. P., Reddy, G. R., and Marnett, L. J. (1996) Relative contribution of cytosine deamination and error-prone replication to the induction of propanodeoxyguanosine→deoxyadenosine mutations in Escherichia coli. *Chem. Res. Toxicol. 9*, 277–283.
24. Yang, W., and Woodgate, R. (2007) What a difference a decade makes: insights into translesion DNA synthesis. *Proc. Natl. Acad. Sci. U.S.A. 104*, 15591–15598.
25. Lee, C. H., Chandani, S., and Loechler, E. L. (2006) Homology modeling of four Y-family, lesion-bypass DNA polymerases: the case that E. coli Pol IV and human Pol kappa are orthologs, and E. coli Pol V and human Pol eta are orthologs. *J. Mol. Graphics Modell. 25*, 87–102.
26. Minko, I. G., Washington, M. T., Kanuri, M., Prakash, L., Prakash, S., and Lloyd, R. S. (2003) Translesion synthesis past acrolein-derived DNA adduct, gamma-hydroxypropanodeoxyguanosine, by yeast and human DNA polymerase eta. *J. Biol. Chem. 278*, 784–790.
27. Sanchez, A. M., Minko, I. G., Kurtz, A. J., Kanuri, M., Moriya, M., and Lloyd, R. S. (2003) Comparative evaluation of the bioreactivity and mutagenic spectra of acrolein-derived alpha-HOPdG and gamma-HOPdG regioisomeric deoxyguanosine adducts. *Chem. Res. Toxicol. 16*, 1019–1028.
28. Wang, H., Kozekov, I. D., Kozekova, A., Tamura, P. J., Marnett, L. J., Harris, T. M., and Rizzo, C. J. (2006) Site-specific synthesis of oligonucleotides containing malondialdehyde adducts of deoxyguanosine and deoxyadenosine via a postsynthetic modification strategy. *Chem. Res. Toxicol. 19*, 1467–1474.
29. Zang, H., Goodenough, A. K., Choi, J. Y., Irimia, A., Loukachevitch, L. V., Kozekov, I. D., Angel, K. C., Rizzo, C. J., Egli, M., and Guengerich, F. P. (2005) DNA adduct bypass polymerization by Sulfolobus solfataricus DNA polymerase Dpo4: analysis and crystal structures of multiple base pair substitution and frameshift products with the adduct 1,N2-ethenoguanine. *J. Biol. Chem. 280*, 29750–29764.
30. Johnson, R. E., Washington, M. T., Prakash, S., and Prakash, L. (2000) Fidelity of human DNA polymerase eta. *J. Biol. Chem. 275*, 7447–7450.
31. Creighton, S., Bloom, L. B., and Goodman, M. F. (1995) Gel fidelity assay measuring nucleotide misinsertion, exonucleolytic proofreading, and lesion bypass efficiencies. *Methods Enzymol. 262*, 232–256.
32. Mendelman, L. V., Petruska, J., and Goodman, M. F. (1990) Base mispair extension kinetics. Comparison of DNA polymerase alpha and reverse transcriptase. *J. Biol. Chem. 265*, 2338–2346.
33. Shibutani, S., Takeshita, M., and Grollman, A. P. (1991) Insertion of specific bases during DNA synthesis past the oxidation-damaged base 8-oxodG. *Nature 349*, 431–434.
34. Choi, J. Y., Chowdhury, G., Zang, H., Angel, K. C., Vu, C. C., Peterson, L. A., and Guengerich, F. P. (2006) Translesion synthesis across O6-alkylguanine DNA adducts by recombinant human DNA polymerases. *J. Biol. Chem. 281*, 38244–38256.
35. Kamiya, H. (2003) Mutagenic potentials of damaged nucleic acids produced by reactive oxygen/nitrogen species: approaches using synthetic oligonucleotides and nucleotides: survey and summary. *Nucleic Acids Res. 31*, 517–531.
36. Johnson, R. E., Trincao, J., Aggarwal, A. K., Prakash, S., and Prakash, L. (2003) Deoxynucleotide triphosphate binding mode conserved in Y family DNA polymerases. *Mol. Cell. Biol. 23*, 3008–3012.
37. Trincao, J., Johnson, R. E., Escalante, C. R., Prakash, S., Prakash, L., and Aggarwal, A. K. (2001) Structure of the catalytic core of S. cerevisiae DNA polymerase eta: implications for translesion DNA synthesis. *Mol. Cell 8*, 417–426.
38. Fuchs, R. P., Koffel-Schwartz, N., Pelet, S., Janel-Bintz, R., Napolitano, R., Becherel, O. J., Broschard, T. H., Burnouf, D. Y., and Wagner, J. (2001) DNA polymerases II and V mediate respectively mutagenic (−2 frameshift) and error-free bypass of a single N-2-acetylaminofluorene adduct. *Biochem. Soc. Trans. 29*, 191–195.
39. Napolitano, R., Janel-Bintz, R., Wagner, J., and Fuchs, R. P. (2000) All three SOS-inducible DNA polymerases (Pol II, Pol IV and Pol V) are involved in induced mutagenesis. *EMBO J. 19*, 6259–6265.
40. Haracska, L., Yu, S. L., Johnson, R. E., Prakash, L., and Prakash, S. (2000) Efficient and accurate replication in the presence of 7,8-dihydro-8-oxoguanine by DNA polymerase eta. *Nat. Genet. 25*, 458–461.
41. Washington, M. T., Johnson, R. E., Prakash, S., and Prakash, L. (1999) Fidelity and processivity of Saccharomyces cerevisiae DNA polymerase eta. *J. Biol. Chem. 274*, 36835–36838.
42. Washington, M. T., Johnson, R. E., Prakash, S., and Prakash, L. (2000) Accuracy of thymine-thymine dimer bypass by Saccharomyces cerevisiae DNA polymerase eta. *Proc. Natl. Acad. Sci. U.S.A. 97*, 3094–3099.
43. Washington, M. T., Johnson, R. E., Prakash, S., and Prakash, L. (2001) Mismatch extension ability of yeast and human DNA polymerase eta. *J. Biol. Chem. 276*, 2263–2266.

44. Washington, M. T., Johnson, R. E., Prakash, L., and Prakash, S. (2001) Accuracy of lesion bypass by yeast and human DNA polymerase eta. *Proc. Natl. Acad. Sci. U.S.A. 98*, 8355–8360.
45. Masutani, C., Kusumoto, R., Iwai, S., and Hanaoka, F. (2000) Mechanisms of accurate translesion synthesis by human DNA polymerase eta. *EMBO J. 19*, 3100–3109.
46. Carlson, K. D., and Washington, M. T. (2005) Mechanism of efficient and accurate nucleotide incorporation opposite 7,8-dihydro-8-oxoguanine by Saccharomyces cerevisiae DNA polymerase eta. *Mol. Cell. Biol. 25*, 2169–2176.
47. Choi, J. Y., and Guengerich, F. P. (2005) Adduct size limits efficient and error-free bypass across bulky N2-guanine DNA lesions by human DNA polymerase eta. *J. Mol. Biol. 352*, 72–90.
48. Choi, J. Y., Zang, H., Angel, K. C., Kozekov, I. D., Goodenough, A. K., Rizzo, C. J., and Guengerich, F. P. (2006) Translesion synthesis across 1,N2-ethenoguanine by human DNA polymerases. *Chem. Res. Toxicol. 19*, 879–886.
49. de los Santos, C., Zaliznyak, T., and Johnson, F. (2001) NMR characterization of a DNA duplex containing the major acrolein-derived deoxyguanosine adduct gamma-OH-1,-N2-propano-2′-deoxyguanosine. *J. Biol. Chem. 276*, 9077–9082.
50. Stone, M. P., Cho, Y. J., Huang, H., Kim, H. Y., Kozekov, I. D., Kozekova, A., Wang, H., Minko, I. G., Lloyd, R. S., Harris, T. M., and Rizzo, C. J. (2008) Interstrand DNA cross-links induced by alpha,beta-unsaturated aldehydes derived from lipid peroxidation and environmental sources. *Acc. Chem. Res. 41*, 793–804.
51. Riggins, J. N., Daniels, J. S., Rouzer, C. A., and Marnett, L. J. (2004) Kinetic and thermodynamic analysis of the hydrolytic ring-opening of the malondialdehyde-deoxyguanosine adduct, 3-(2′-deoxy-beta-D-erythro-pentofuranosyl)-pyrimido[1,2-alpha]purin-10(3H)-one. *J. Am. Chem. Soc. 126*, 8237–8243.
52. Riggins, J. N., Pratt, D. A., Voehler, M., Daniels, J. S., and Marnett, L. J. (2004) Kinetics and mechanism of the general-acid-catalyzed ring-closure of the malondialdehyde-DNA adduct, N2-(3-oxo-1-propenyl)deoxyguanosine (N2OPdG-), to 3-(2′-deoxy-beta-D-erythro-pentofuranosyl)pyrimido[1,2-alpha]purin-10(3H)-one (M1dG). *J. Am. Chem. Soc. 126*, 10571–10581.
53. Lukin, M., and de los Santos, C. (2006) NMR structures of damaged DNA. *Chem. Rev. 106*, 607–686.
54. Nechev, L. V., Kozekov, I. D., Brock, A. K., Rizzo, C. J., and Harris, T. M. (2002) DNA adducts of acrolein: site-specific synthesis of an oligodeoxynucleotide containing 6-hydroxy-5,6,7,8-tetrahydropyrimido[1,2-a]purin-10(3H)-one, an acrolein adduct of guanine. *Chem. Res. Toxicol. 15*, 607–613.
55. Washington, M. T., Minko, I. G., Johnson, R. E., Haracska, L., Harris, T. M., Lloyd, R. S., Prakash, S., and Prakash, L. (2004) Efficient and error-free replication past a minor-groove N2-guanine adduct by the sequential action of yeast Rev1 and DNA polymerase zeta. *Mol. Cell. Biol. 24*, 6900–6906.
56. Washington, M. T., Minko, I. G., Johnson, R. E., Wolfle, W. T., Harris, T. M., Lloyd, R. S., Prakash, S., and Prakash, L. (2004) Efficient and error-free replication past a minor-groove DNA adduct by the sequential action of human DNA polymerases iota and kappa. *Mol. Cell. Biol. 24*, 5687–5693.

BI801591A